

# Photoreversible Surfaces to Regulate Cell Adhesion

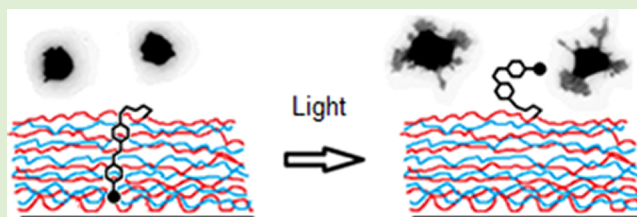
Alexis Goulet-Hanssens,<sup>†</sup> Karen Lai Wing Sun,<sup>‡</sup> Timothy E. Kennedy,<sup>‡</sup> and Christopher J. Barrett<sup>\*†</sup>

<sup>†</sup>Department of Chemistry, Program in NeuroEngineering, McGill University, 801 Sherbrooke Street West, Montreal, Quebec, Canada H3A 0B8

<sup>‡</sup>Department of Neurology and Neurosurgery, Program in NeuroEngineering, Montreal Neurological Institute, 3801 University Street, Montreal, Quebec, Canada H3A 2B4

## S Supporting Information

**ABSTRACT:** We report the development of a photo-reversible cell culture substrate. We demonstrate the capacity to modify the adhesivity of the substrate using light, altering its capacity to support cell growth. Polyelectrolyte multilayers (PEMs) were used to produce tunable substrates of different thickness and matrix stiffness, which have different intrinsic capacities to support cell adhesion and survival. Surfaces were top-coated with a poly(acrylic acid)-poly(allylamine hydrochloride) polyelectrolyte bilayer functionalized with a small fraction (<1%) of an azobenzene-based photoswitchable sidegroup, which included the cell-adhesive three-amino-acid peptide RGD. Irradiation with light-induced geometric switching of the azo bond, resulting in changes to RGD exposure and consequently to cell adhesion and survival, was investigated on a variety of surfaces of different thickness and stiffness. Substrate stiffness, as modified by the thickness, had a significant influence on the adhesion of NIH 3T3 cells, consistent with previous studies. However, by disrupting the isomerization state of the azobenzene-linked RGD and exposing it to the surface, cell adhesion and survival could be enhanced up to 40% when the positioning of the RGD peptide was manipulated on the softest substrates. These findings identify permissive, yet less-than-optimal, cell culture substrate conditions that can be substantially enhanced using noninvasive modification of the substrate triggered by light. Indeed, where cell adhesion was tuned to be suboptimal under baseline conditions, the light-induced triggers displayed the most enhanced effect, and identification of this ‘Goldilocks zone’ was key to enabling light triggering.



## INTRODUCTION

Cell adhesion and growth on a surface is influenced by complex molecular mechanisms that regulate the interaction of cells with the local physical and chemical environment. The integrin family of transmembrane proteins are major receptors for extracellular matrix (ECM) components, such as fibronectin and laminins,<sup>1</sup> and many cell types respond to the physical properties of their environment through integrin-mediated adhesions. Integrin intracellular domains form complexes with cytoplasmic proteins such as talin, paxillin, vinculin, and kindlin that locally direct the organization of the cytoskeleton.<sup>2,3</sup> By binding ECM proteins extracellularly and being linked to the intracellular cytoskeleton, integrins form critical force transducing links across the cellular plasma membrane. Of the various ECM proteins, fibronectin-mediated adhesion can be mimicked by a remarkably small tripeptide sequence composed of arginine, glycine, and aspartic acid: RGD.<sup>4,5</sup> The affinity of this peptide sequence to bind integrins can be increased by the addition of one extra hydrophobic residue<sup>6</sup> or by cyclization, which mimics the native  $\beta$ -turn present in full-length fibronectin.<sup>7</sup>

In addition to biochemical receptor–ligand interactions, physical qualities – such as surface layer hardness, moisture content, and surface charge – also influence the capacity of a substrate to promote cell adhesion and survival.<sup>8,9</sup> Tailoring the material properties of the culture surface can critically influence

cell survival.<sup>10</sup> Polyelectrolyte multilayers (PEMs) are versatile, effective, and relatively simple materials to engineer thin films with defined properties.<sup>11,12</sup> Sequential deposition of charged polymers on a charged substrate (clean silicon or glass) results in the formation of films of variable thickness and softness that can be controlled by varying the charge density of the polymer chains being deposited, which can be controlled by the pH of the polymer solution used during deposition.<sup>13</sup> A recent report on the preparation of 2-D gradient PEM films for cell viability studies provides an efficient technique for combinatorial screening of many thousands of conditions on a single cell culture surface.<sup>14,15</sup>

Obtaining more precise control over cell adhesion and morphology remains an important challenge for biomaterials engineering.<sup>16,17</sup> Materials and techniques that provide control over surface properties have made use of a number of external stimuli as triggers, including light,<sup>18,19</sup> electrical,<sup>20,21</sup> pH,<sup>22,23</sup> and thermal.<sup>24,25</sup> Among these stimuli, light is advantageous, allowing for localized and high-resolution control over the cell-material interface and low interference with normal biological function. Furthermore, the incorporation of light-sensitive chemical photoswitches, such as the trans–cis isomerization

Received: July 5, 2012

Revised: August 21, 2012

Published: August 22, 2012

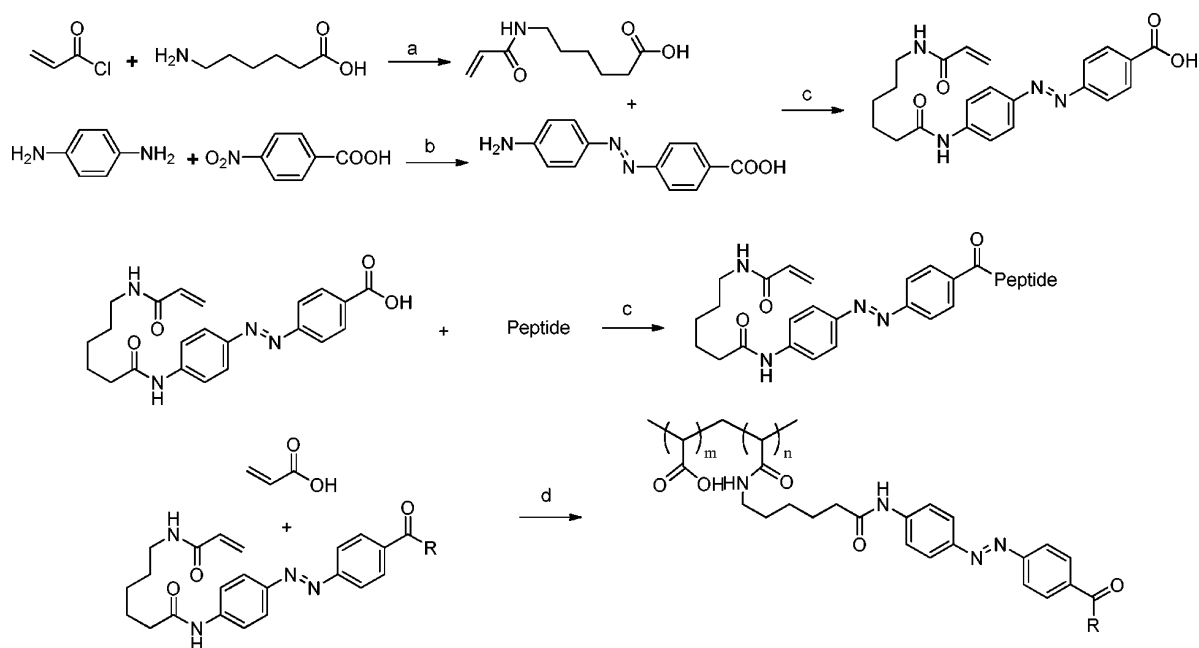


**Figure 1.** Synthesis of azobenzene-*co*-acrylic acid polymers for photoresponsive topcoat. (a) NaOH, H<sub>2</sub>O, 0 °C. (b) NaOH, H<sub>2</sub>O, 95 °C, 16 h. (c) HATU, collidine, DMF, 25 °C. (d) AIBN, DMF 80 °C. In this case, R can be OH, RGD, or c(RGDfK). *m/n* ratios are approximately 100:1.

of azobenzene, can provide reversible control over the properties of a surface by switching between relatively growth permissive and nonpermissive surface states.

Incorporating the tripeptide RGD into an azobenzene can be used to harness and control the affinity of this ligand for its receptor.<sup>26,27</sup> Azobenzene-mediated photocontrol of cell adhesion has been demonstrated on substrates of silicon<sup>28</sup> and gold<sup>29</sup> using azobenzene-tethered RGD ligands anchored to the substrate. However, these previous studies have been limited, having offered no control over the physical properties of the surface to which the cells adhere. We now demonstrate the combination of photoswitched surface cytophilicity and tailored surfaces with the goal of elucidating conditions for maximizing photo switching. Here the RGD was incorporated at a low concentration, less than a 1:100 ratio in an acrylic acid copolymer, yet still functions as a powerful reversible trigger of biological activity. Also, the key to the photoswitchable utility of this material is the concurrent ability to tune the baseline matrix conditions, choosing those that are only moderately adhesive, so that the switch occurs in a regime that will effect the greatest change with light.

## MATERIALS AND METHODS

With the exception of HATU (EMD Novabiochem, Hohenbrunn, Germany) and c(RGDfK) (21st century biochemicals, Marlboro, MA), all chemicals were purchased from Aldrich corporation (St. Louis, MO). The azo monomers: *N*-acryloyl-6-aminohexanoic-(4-aminophenyl)azo-4-benzoic acid, acryloyl-ahx-(4-aminophenyl)azo-4-benzocarbonyl-RGD, and acryloyl-ahx-(4-aminophenyl)azo-4-benzocarbonyl-c(-RGDfK-) were synthesized with slight modifications from the literature.<sup>28,30</sup> Detailed synthetic procedures can be found in the Supporting Information. The prepared azo-monomers were then copolymerized with freshly distilled acrylic acid in dry dimethylformamide (DMF; refluxed and distilled from CaH<sub>2</sub>) initiated by azobisisobutyronitrile (AIBN; recrystallized from methanol, 30 °C). Solutions were placed in custom-made rota-flo polymer-

ization ampules and degassed by three freeze–pump–thaw cycles backfilled with nitrogen and sealed. Polymerizations were thermally initiated at 60 °C, mixed by brief swirling every 6–10 h for 3 days. After polymerization, the polymers were precipitated with a 20:1 excess of diisopropyl ether and left to stir overnight. The three resulting copolymers were found to have an azobenzene content of 1.4 mol % for the *N*-acryloyl-6-aminohexanoic-(4-aminophenyl)azo-4-benzoic acid, 0.21 mol % for the acryloyl-ahx-(4-aminophenyl)azo-4-benzocarbonyl-RGD, and 0.27 mol % for the acryloyl-ahx-(4-aminophenyl)azo-4-benzocarbonyl-c(-RGDfK-), as determined by UV/vis spectroscopy. The solution was filtered and the recovered polymer was redissolved in water to an approximate concentration of 0.1 g/L.

Polyelectrolyte solutions of poly(allylamine)hydrochloride (PAH) (56 000 MW) and poly(acrylic acid) (PAA) (15 000 MW) were prepared in Milli-Q water at a monomer concentration of 0.01 M. Once dissolved, the pH values of the solutions were adjusted to the desired acidity using 1 M NaOH or HCl solutions. Flat silicon and glass surfaces approximately 2.5 cm<sup>2</sup> in area were placed in a ‘piranha’ cleaning bath (2:1 18 M sulfuric acid/30% hydrogen peroxide) at boiling for 30 min to clean and render a negative surface charge. The cleaned silica surfaces were rinsed thoroughly with Milli-Q water and dipped alternately in the PAH and PAA solutions to yield 13 multilayers and a terminal positive charge, a number of layers determined through previous studies to be near optimal to promote cell adhesion and survival.<sup>14</sup> The material control wafers were dipped one final time into the PAA solution while the three different photoresponsive surfaces were dipped into the desired azo-*co*-polymer solution. Thicknesses of all films were measured from hydrated films using a single wavelength null-ellipsometer (633 nm. Optrel, Multiskop).

To initiate isomerization, surfaces were irradiated with a Blak-ray lamp (UVP, Upland, CA) with emission centered at 365 nm at a distance of 20 cm from the samples with a power

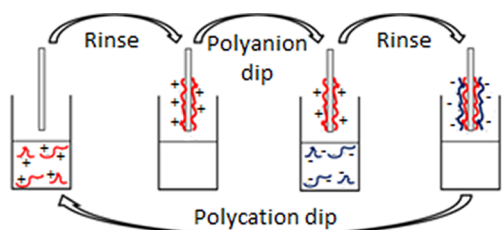


**Figure 2.** Illustration of dipping process, beginning with a negatively charged substrate (glass or silicon) being dipped in a polycation solution.

of 12 mW/cm<sup>2</sup>. For biological experiments, half of each wafer was covered with a silicon mask, preventing isomerization, while the other half was irradiated. After 1 h, the surface had achieved the photostationary state. These half-activated, half-inactivated surfaces were then used immediately for cell culture studies in the 1 to 2 h window while the *cis*-azo population was still near its maximum (a minimum of 75% *cis* content).

NIH 3T3 cells were cultured in Dulbecco's modified Eagle's medium (DMEM) supplemented with 10% heat-inactivated calf serum, 100 unit/mL penicillin G, and 100 μg/mL streptomycin. For experiments, cells were trypsinized and resuspended in serum-free DMEM. DiI<sub>18</sub>(3) (DiI, 25 uL) solution (Invitrogen, Carlsbad, CA) was added to the cell suspension and incubated at 37 °C for 30 min to label cell membranes. The cells were then pelleted and resuspended in 10 mL of serum-free DMEM to achieve a concentration of ~82 000 cells/mL.

Freshly irradiated surfaces were placed in a 60 mm culture dish with 1 mL of the DiI-labeled cell suspension and 3 mL of serum-free DMEM, incubated for 30 min. Cells were imaged using an Axioskop2 microscope (Carl Zeiss, Toronto, Canada) with 532 nm fluorescence at 10× magnification. Ten separate images were captured at both 30 and 60 min after plating: five from the irradiated side and five from the nonirradiated portion of the surface for each time point, for a total of 20 images for each of the 12 substrates, for each duplicate. Images were analyzed using ImageJ (NIH)<sup>31</sup> software to calculate average cell surface area. Two-way ANOVAs with Bonferroni post-tests were performed using Graphpad Prism 5.

## RESULTS AND DISCUSSION

In this study, surfaces with pH assembly conditions of PAH pH 8.5 and PAA pH 5, 6, and 7 containing 14 layers were generated because these conditions appeared to support cell survival and surface switching.<sup>14</sup> The pH of assembly has a predictable and reproducible effect on substrate stiffness<sup>14</sup> as well as other material properties, which can exert a significant influence on determining cell survival on a surface.<sup>32</sup> On the basis of these previous studies, evidence of cell viability on a PEM substrate becomes apparent within a 60 min time scale. In our study, cell surface area was considered to be a good correlate of the extent of cell-substrate adhesion.

**Table 1.** Polyelectrolyte Assembly Conditions and Resulting Coating Thickness

PAH assembly	PAA assembly	thickness
pH 8.5	pH 5 (weak)	1075 Å
pH 8.5	pH 6 (moderate)	180 Å
pH 8.5	pH 7 (strong)	63 Å

Surfaces were irradiated with UV light at 365 nm wavelength for 2 h. After this irradiation time, a saturated photostationary state was achieved with a *cis* content of at least 75%. Kinetic studies were performed in DMF solution and in multilayered films to confirm slow thermal back-isomerization of the *cis*-azobenzene. Kinetic plots of the chromophores in DMF solution show first-order decay with half-lives of 8.4 h for the 4,4' aminophenyl-azobenzoic acid copolymer, 14.9 h for the RGD copolymer, and 21.9 h for the c(RGDfK) copolymer. In PEMs, the decay kinetics deviate slightly from first order, as has been shown to be due to confinement and free volume effects.<sup>33</sup> However, the half-life in the films was still on the order of many hours, implying that the surfaces presented to the cells over the 60 min time-scale of the experiment still contained a high proportion of *cis*-azobenzene.

Results obtained are shown in Figure 4 and summarize experiments performed with films of 12 different surface conditions. Three different layering conditions ranging from thinnest (PAA pH 7, PAH pH 8.5), medium thickness (PAA pH 6, PAH pH 8.5), and thickest (PAA pH 5, PAH pH 8.5) were created, where the PAA is strongly charged, moderately charged, and weakly charged, respectively. These were then top-coated with one of four different functionalities: 1 native polyelectrolyte, 2 photoresponsive with a carboxylic terminated azobenzene, 3 a linear RGD peptide (RGD), or 4 cyclic RGDfK (c(RGDfK)). These 12 surfaces, with 5 images collected of each irradiated and nonirradiated side, at trials of 30 and 60 min, with two full duplicates, comprise an analysis of 4731 cells total under 48 different conditions.

Considering all data sets, the differences in substrate stiffness had the largest impact on cell adhesion and growth. This is consistent with previous reports that the material properties of a substrate are more important than surface charge,<sup>15,32</sup> which can override the presence of a desirable ligand.<sup>34</sup> NIH 3T3 cells are a fibroblast-like cell line and favor stiffer substrates, which are thought to more closely mimic the local environment of fibroblasts in vivo.<sup>35</sup> In all trials, the c(RGDfK)-functionalized surfaces exhibit the greatest cell adhesion, as expected, given the high affinity of α<sub>v</sub>β<sub>III</sub> integrin expressed by NIH 3T3 cells for this surface ligand.<sup>36–38</sup> With surface conditions that are overall less favorable for cell adhesion and growth (PAA pH 5 (weak), Figure 4a), the presentation of ligands and the presence of azobenzene results in a more chemically varied surface and increased cell spreading, suggesting an increase in cell adhesion. The cells are statistically indifferent to irradiation for the control sample, the PEM control, the azo photocontrol, and the cyclic ligand. However, a clear photoinduced 40% increase in cell size was detected after converting to the *cis* form of the linear RGD ligand. Although the difference in ligand availability may not be exactly the same between samples based on the slightly different half lives, the effects we note here run counter to the observed half-lives, namely that the linear RGD should decay fastest and shows the best photoresponse compared with the c(RGDfK) ligand, which shows no photoresponse.

With an increase in the stiffness of the substrate (Figure 4b (moderate)), the photoswitching control exhibited by the linear RGD material was lost, whereas photoswitched cell adhesion increases became apparent with the cyclic ligand. With the stiffest substrates (pH7 PAA (strong) Figure 4c), a threshold was observed where the substrate conditions are so favorable that even the addition of c(RGDfK) ligand does not significantly improve cell adhesion and growth. The presence of the linear RGD ligand results in smaller cells than that of the

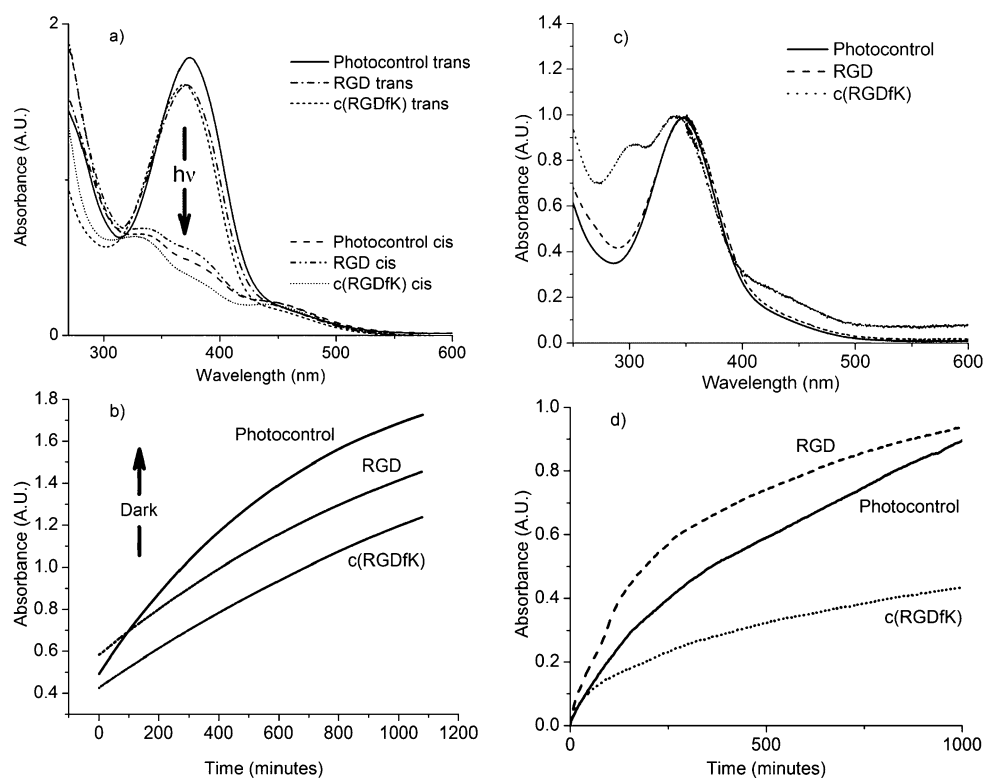


**Figure 3.** (a) Normalized UV/vis spectra of azo polymers in DMF solution showing decrease of the trans isomer on irradiation, (b) kinetics of the return of the cis isomer in the dark, (c) UV/vis spectra of 18 bilayer multilayer polymer films assembled at pH 7, and (d) film trans isomer return kinetics. All kinetic curves were collected at the  $\lambda_{\text{max}}$  of the chromophore being studied after 2 h of blak-ray irradiation, under the same setup as used in the cell experiments.

c(RGDfK) but still leads to a photoinduced 20% increase in cell size. The marked difference in the adhesion and growth of cells plated on the linear RGD versus other substrates may be due to engaging different adhesive mechanisms; elucidating the underlying molecular differences will be an important goal for future studies.

Photoswitching with c(RGDfK) peptides provided the largest contrast in cell adhesion on hard substrates given the high affinity of the cyclic peptide for  $\alpha_v\beta_{III}$  integrin expressed by NIH 3T3 cells. Even at these low ligand densities of <1%, cells appear to respond strongly to the presence of this ligand.<sup>39</sup> This effect likely underlies the observation that despite the greater ligand affinity, high cell adhesion and growth with very little photoenhancement is observed in these films. Although photoswitching surfaces with tethered azobenzene peptides have been previously reported,<sup>28,29</sup> these former studies were exclusively conducted by placing the ligand on a stiff bioinert substrate and counting on the decreased tether length of the cis azobenzene to reduce the availability of the ligand to trigger integrin-mediated adhesion. The reproducible trend observed points to an opposite effect in multilayered thin films incorporating these azobenzene peptides, where the isomerized species leads to an increase in cell adhesion. This effect can be rationalized by the zwitterionic RGD peptide itself being potentially layered into the film due to the strong interactions that are expected between the peptide and the soft, wet, ionic, and hydrogen bonding environment of these PEM biofilms, permitting ligand penetration into the film. The azobenzene isomerization from trans to cis then disrupts this affinity penetration and releases the ligand from the multilayer, making it available for integrin recognition and leading to the observed

enhanced cell spreading. A simple cartoon schematic of this proposed mechanism is presented in Figure 5 as an illustrative aid for visualization.

As is typical of all azobenzene derivatives, the surface can be reversibly switched many times from trans to cis with little to no loss of chromophore response; this photostability can easily be measured spectroscopically over numerous trans–cis–trans cycles. However, once the multilayers are placed in contact with cells, the charged nature of the surface leads to irreversible binding of extracellular and ECM proteins, thereby preventing the use of the clean surface in future cell experiments. Given the long time frame of thermal cis–trans isomerization, it is possible that the reduction in cell adhesion observed in the trans substrates results from the ligand readsorbing into the PEM, as opposed to the isomerization state of the azobenzene. Nevertheless, light-driven isomerization from trans to cis of select azobenzene-tethered ligands results in clear and significant photoenhanced cell adhesion and growth under the right conditions.

## CONCLUSIONS

In summary, we have synthesized and tested three photoresponsive polyelectrolytes for their capacity to enhance the growth of NIH 3T3 cells on substrates composed of PEMs of different thicknesses when irradiated. Surface layer thickness strongly influenced the extent to which different substrates support cell adhesion and growth, with preferential growth on thinner, stiffer substrates that more closely mimic the cell's natural environment.<sup>35,40</sup> Consistent with previous findings, the c(RGDfK) ligand very effectively promoted cell adhesion, but only to the extent that the induced conformational change did

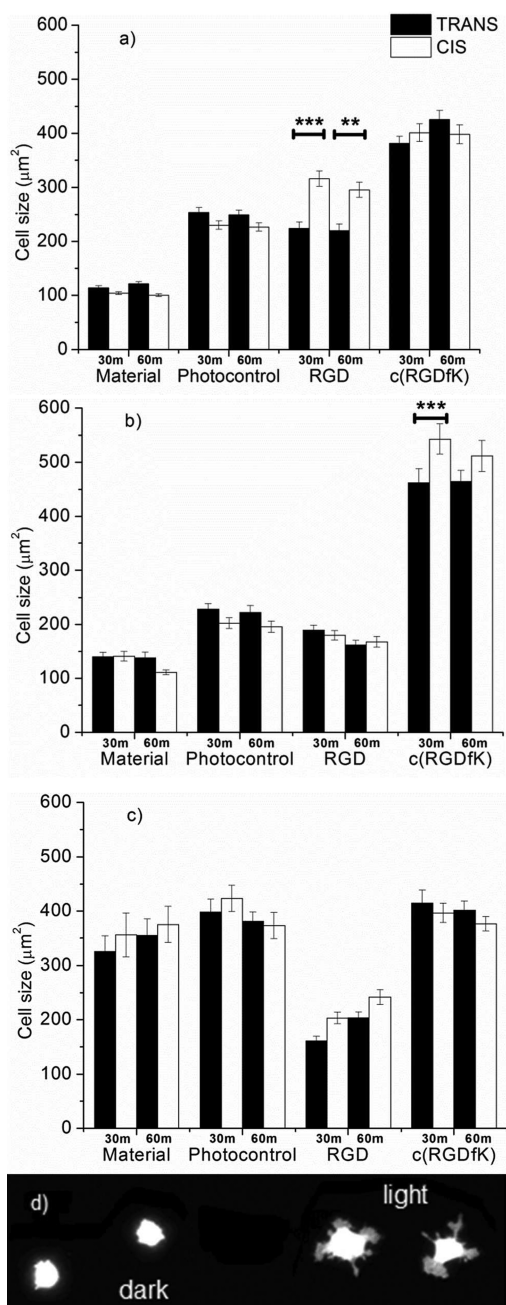


**Figure 4.** Cell size as a function of surface coating and irradiation state of the surface: (a) PAA pH 5 (weak) film (\*\*\*,  $p < 0.001$ ; \*\*,  $p < 0.01$ ), (b) PAA pH 6 (moderate) film, and (c) PAA pH 7 (strong) film. (d) Representative increase in cell surface area without and with surface irradiation.

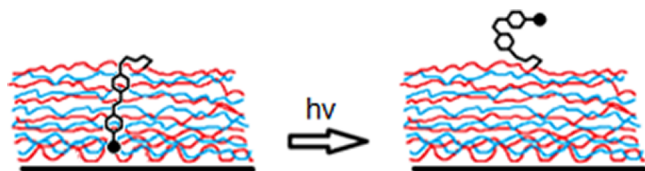


**Figure 5.** Potential mechanism for enhanced cell adhesion, where the geometric isomerization upon irradiation disrupts the 'buried' configuration of the RGD and exposes it to the surface and adjacent cells.

not further enhance growth on the substrate. Cells grown on a less-than-optimal, yet relatively moderately hospitable substrate exhibited the greatest photoenhanced growth, with a ~40% increase in size after 30 min. We describe this as a 'Goldilocks zone', in which the capacity of the substrate to support cell adhesion is tuned to be permissive, yet is sufficiently suboptimal that the light-induced trigger results in substantial enhancement of cell adhesion. Coupling the capacity to photoactivate the substrate with the diversity of possible surface properties generated using PEMs provides a significant parameter space for fine-tuning of tailored biosurfaces with good control. These materials and this technique in combination thus have utility as an experimental tool for evaluating how a wide range of surface conditions may influence cell adhesion and growth and possibly to use photoactivated tuning as a technique to direct cell migration or to manipulate even more localized dynamic behavior, such as directing neurite outgrowth unidirectionally.

## ■ ASSOCIATED CONTENT

### § Supporting Information

Synthesis of intermediates as well as NMR and mass spectrometry data of compounds is detailed. This material is available free of charge via the Internet at <http://pubs.acs.org>.

## ■ AUTHOR INFORMATION

### Corresponding Author

\*E-mail: [christopher.barrett@mcgill.ca](mailto:christopher.barrett@mcgill.ca).

### Notes

The authors declare no competing financial interest.

## ■ ACKNOWLEDGMENTS

Supported by a New Emerging Team grant from CIHR to T.E.K and C.J.B. and an NSERC CREATE Training Grant in support of the McGill Program in NeuroEngineering, and an operating grant #FRN79513 to T.E.K. from the Canadian Institutes of Health Research (CIHR). A.G.H. wishes to thank FQRNT for a B2 Doctoral Scholarship. K.L.W.S. was supported by a Jeanne-Timmins Costello Graduate Fellowship. T.E.K. is a Killam Foundation Scholar and holds a Chercheur National award from the Fonds de la Recherche en Santé du Québec.

## ■ ABBREVIATIONS

c(RGDfK), cyclic peptide arginine-glycine-aspartic acid-L-phenylalanine-lysine; DiI, 1,1'-dioctadecyl-3,3,3',3'-tetramethylindocarbocyanine perchlorate; ECM, extracellular matrix; PAA, poly(acrylic acid); PAH, poly(allylamine hydrochloride); PEM, polyelectrolyte multilayer; RGD, arginine-glycine-aspartic acid

## ■ REFERENCES

- (1) Hynes, R. O. *Cell* **2002**, *110*, 673–687.
- (2) Moser, M.; Legate, K. R.; Zent, R.; Fässler, R. *Science* **2009**, *324*, 895–899.
- (3) Bökel, C.; Brown, N. H. *Dev. Cell* **2002**, *3*, 311–321.
- (4) Pierschbacher, M. D.; Ruoslahti, E. *Nature* **1984**, *309*, 30–33.
- (5) Hautanen, A.; Gailit, J.; Mann, D. M.; Ruoslahti, E. *J. Biol. Chem.* **1989**, *264*, 1437–1442.
- (6) Park, H. S.; Kim, C.; Kang, Y. K. *Biopolymers* **2002**, *63*, 298–313.
- (7) Koivunen, E.; Wang, B.; Ruoslahti, E. *Nat. Biotechnol.* **1995**, *13*, 265–270.
- (8) Hern, D. L.; Hubbell, J. A. *J. Biomed. Mater. Res.* **1998**, *39*, 266–276.

- (9) Auernheimer, J.; Zukowski, D.; Dahmen, C.; Kantlehner, M.; Enderle, A.; Goodman, S. L.; Kessler, H. *ChemBioChem* **2005**, *6*, 2034–2040.
- (10) Hubbell, J. A. *Curr. Opin. Biotechnol.* **2003**, *14*, 551–558.
- (11) Elbert, D. L.; Herbert, C. B.; Hubbell, J. A. *Langmuir* **1999**, *15*, 5355–5362.
- (12) Ren, K.; Crouzier, T.; Roy, C.; Picart, C. *Adv. Funct. Mater.* **2008**, *18*, 1378–1389.
- (13) Dubas, S. T.; Schlenoff, J. B. *Macromolecules* **1999**, *32*, 8153–8160.
- (14) Sailer, M.; Barrett, C. J. *Macromolecules* **2012**, *45*, 5704–5711.
- (15) Sailer, M.; Lai Wing Sun, K.; Mermut, O.; Kennedy, T. E.; Barrett, C. J. *Biomaterials* **2012**, *33*, 5841–5847.
- (16) Martino, M. M.; Mochizuki, M.; Rothenfluh, D. A.; Rempel, S. A.; Hubbell, J. A.; Barker, T. H. *Biomaterials* **2009**, *30*, 1089–1097.
- (17) Marklein, R. A.; Burdick, J. A. *Adv. Mater.* **2010**, *22*, 175–189.
- (18) Petersen, S.; Alonso, J. M.; Specht, A.; Duodu, P.; Goeldner, M.; del Campo, A. *Angew. Chem., Int. Ed.* **2008**, *47*, 3192–3195.
- (19) Ohmuro-Matsuyama, Y.; Tatsu, Y. *Angew. Chem., Int. Ed.* **2008**, *47*, 7527–7529.
- (20) Abidian, M. R.; Ludwig, K. A.; Marzullo, T. C.; Martin, D. C.; Kipke, D. R. *Adv. Mater.* **2009**, *21*, 3764–3770.
- (21) Saltó, C.; Saindon, E.; Bolin, M.; Kanciurzevska, A.; Fahlman, M.; Jager, E. W. H.; Tengvall, P.; Arenas, E.; Berggren, M. *Langmuir* **2008**, *24*, 14133–14138.
- (22) Yu, X.; Wang, Z.; Jiang, Y.; Shi, F.; Zhang, X. *Adv. Mater.* **2005**, *17*, 1289–1293.
- (23) Burke, S. E.; Barrett, C. J. *Biomacromolecules* **2003**, *4*, 1773–1783.
- (24) Spruell, J. M.; Wolffs, M.; Leibfarth, F. a; Stahl, B. C.; Heo, J.; Connal, L. a; Hu, J.; Hawker, C. J. *J. Am. Chem. Soc.* **2011**, *133*, 16698–16706.
- (25) Xu, J.; Song, J. In *Biomedical Engineering - Frontiers and Challenges*; Fazel-Rezai, R., Ed.; Intech: New York, 2011; pp 125–142.
- (26) Milbradt, A. G.; Löweneck, M.; Krupka, S. S.; Reif, M.; Sinner, E.-K.; Moroder, L.; Renner, C. *Biopolymers* **2005**, *77*, 304–313.
- (27) Schütt, M.; Krupka, S. S.; Milbradt, A. G.; Deindl, S.; Sinner, E.-K.; Oesterheld, D.; Renner, C.; Moroder, L. *Chem. Biol.* **2003**, *10*, 487–490.
- (28) Auernheimer, J.; Dahmen, C.; Hersel, U.; Bausch, A.; Kessler, H. *J. Am. Chem. Soc.* **2005**, *127*, 16107–16110.
- (29) Liu, D.; Xie, Y.; Shao, H.; Jiang, X. *Angew. Chem., Int. Ed.* **2009**, *48*, 4406–4408.
- (30) Bentolila, A.; Vlodaysky, I.; Ishai-Michaeli, R.; Kovalchuk, O.; Haloun, C.; Domb, A. J. *J. Med. Chem.* **2000**, *43*, 2591–2600.
- (31) Abràmoff, M. D.; Magalhães, P. J.; Sunanda, R. J. *Biophotonics Int.* **2004**, *11*, 36–42.
- (32) Mendelsohn, J. D.; Yang, S. Y.; Hiller, J.; Hochbaum, A. I.; Rubner, M. F. *Biomacromolecules* **2003**, *4*, 96–106.
- (33) Barrett, C.; Natansohn, A.; Rochon, P. *Chem. Mater.* **1995**, *7*, 899–903.
- (34) Picart, C.; Elkaim, R.; Richert, L.; Audoin, F.; Arntz, Y.; Da Silva Cardoso, M.; Schaaf, P.; Voegel, J.-C.; Frisch, B. *Adv. Funct. Mater.* **2005**, *15*, 83–94.
- (35) Levental, I.; Georges, P. C.; Janmey, P. A. *Soft Matter* **2007**, *3*, 299–306.
- (36) Pierschbacher, M. D.; Ruoslahti, E. *J. Biol. Chem.* **1987**, *262*, 17294–17298.
- (37) Heckmann, D.; Kessler, H. In *Methods in Enzymology*; Allis, A. C., Ed.; Academic Press: San Diego, California, 2007; Vol. 426, pp 463–503.
- (38) Hersel, U.; Dahmen, C.; Kessler, H. *Biomaterials* **2003**, *24*, 4385–4415.
- (39) Liu, J. C.; Tirrell, D. A. *Biomacromolecules* **2008**, *9*, 2984–2988.
- (40) Saha, K.; Keung, A. J.; Irwin, E. F.; Li, Y.; Little, L.; Schaffer, D. V.; Healy, K. E. *Biophys. J.* **2008**, *95*, 4426–4438.